

High-Throughput Computational Screening of Hydrocarbon Molecules for Long-Wavelength Infrared Imaging

Maliheh Shaban Tameh, Veaceslav Coropceanu,* Addison G. Coen, Jeffrey Pyun,* Dennis L. Lichtenberger,* and Jean-Luc Brédas*



Cite This: *ACS Materials Lett.* 2024, 6, 4371–4378



Read Online

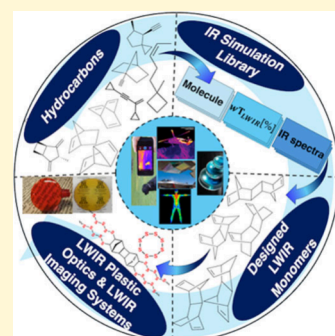
ACCESS |

Metrics & More

Article Recommendations

Supporting Information

ABSTRACT: The development of organic or sulfur/organic hybrid polymeric materials for infrared (IR) thermal imaging applications has attracted significant interest as an alternative to expensive semiconductor transmissive materials, particularly for long-wavelength IR (LWIR, 1250–800 cm⁻¹/8–12.5 μm). To accelerate the design of new candidate IR polymers with enhanced LWIR optical transparency, we have developed a protocol that integrates density functional theory calculations for simulating IR spectra (including both frequencies and absorption intensities of the vibrations) with high-throughput screening. This approach enables us to explore novel hydrocarbon molecules with improved LWIR transmittance which retain reactive groups conducive to polymerization with sulfur. The aim is to incorporate novel candidate molecules with high predicted IR transparency into polymeric materials, namely chalcogenide hybrid sulfur polymers synthesized by the inverse vulcanization of elemental sulfur. Starting from a relatively large library of unsaturated 35,238 hydrocarbons, this study introduces a set of promising candidates whose high LWIR percent window transparency values (*wT*) and chemical structures are expected to produce novel transparent hybrid sulfur/organic plastic materials.



Infrared (IR) imaging is of tremendous technological importance for sensing device systems that have a wide range of applications in the defense and consumer market sectors, particularly in the long-wave infrared (LWIR, 1250–800 cm⁻¹/8–12.5 μm) or midwave infrared (MWIR, 3300–2000 cm⁻¹/3–5 μm) regions.^{1–5} Current state-of-art transmissive materials for IR imaging include mainly gallium arsenide (GaAs), germanium (Ge), arsenic selenide (As₂Se₃), and amorphous chalcogenide glasses,⁶ which have been of interest due to their high transmission and high refractive index across the IR spectrum. However, the high cost and low Earth abundance of these inorganic IR transmissive materials represent major disadvantages for large-scale manufacturing and for the wider deployment of this technology to high-volume markets. In this regard, the use of optical polymeric materials emerges as an attractive alternative due to the lower cost and facile processability of this class of materials versus the current state of the art. However, the intrinsically higher IR absorption of organic molecules due to carbon-based bond vibrations have limited the application of synthetic optical polymers based on hydrocarbon-based molecules for IR optical technologies.

A significant advance to address this technological problem was achieved by Pyun and co-workers through their develop-

ment of high-sulfur-content chalcogenide hybrid inorganic/organic polymers via inverse vulcanization.^{7–10} This new class of optical hybrid polymers exhibits remarkably high refractive index and IR transparency due to the presence of a high content of S–S bonds coupled with a dramatic reduction in IR absorbing organic units, which has prompted significant interest for use in IR imaging and photonics.^{6,9–16} Furthermore, these optical polymers are low cost due to the enormous volume of elemental (S₈) sulfur generated via oil and natural-gas refining processes. In the past decade, the inverse vulcanization process¹⁷ has been expanded to include various types of unsaturated organic monomers including norbornadiene (NBD), triisopropenyl-benzene (TIB),¹⁸ diisopropenyl benzene (DIB),^{17,19} divinylbenzene (DVB), ethylidene norbornene (ENB), vinyl norbornene (VNB), dicyclopentadiene (DCPD),^{20–24} and 1,3,5-trivinylbenzene (TVB).²⁵

Received: May 17, 2024

Revised: August 13, 2024

Accepted: August 13, 2024

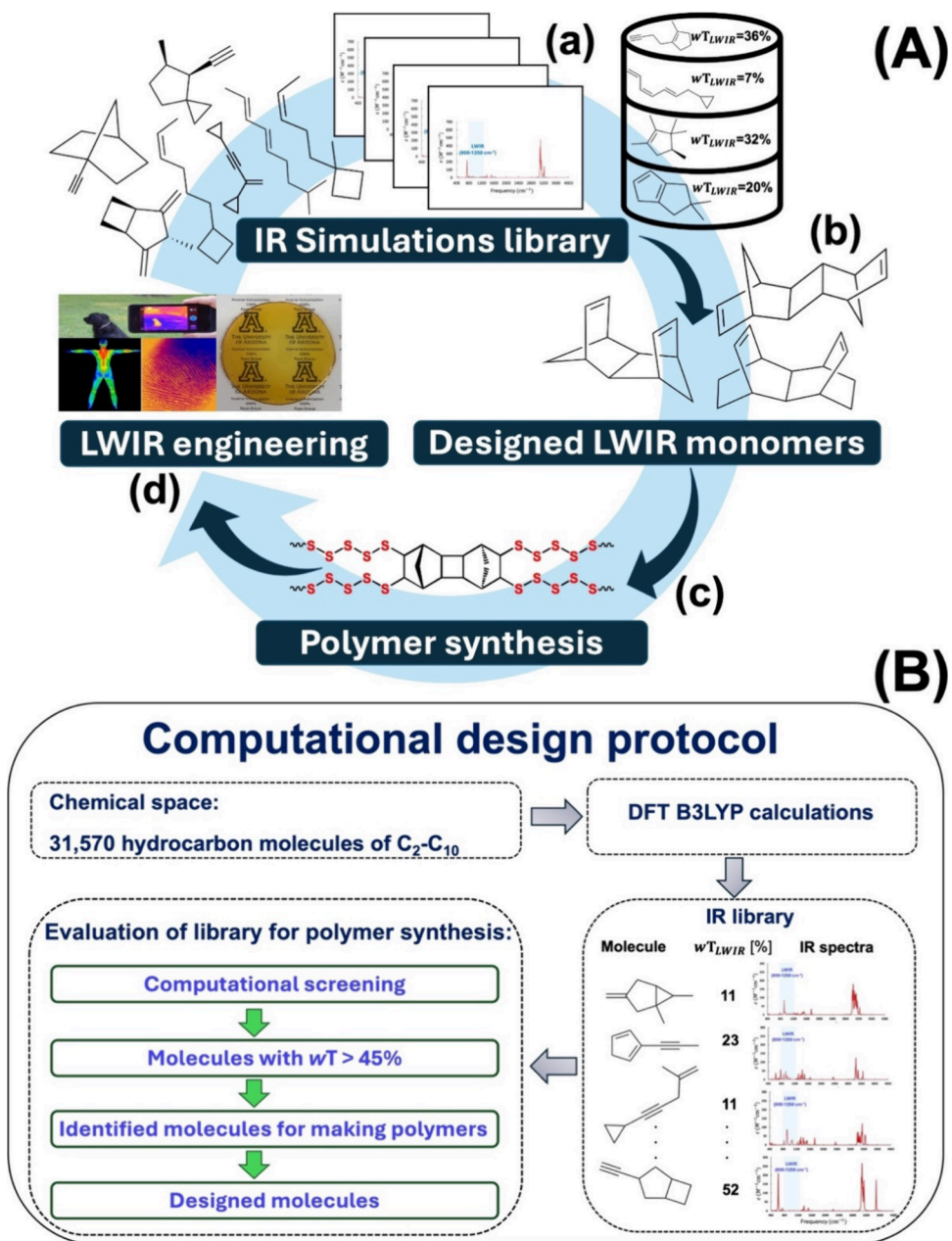


Figure 1. (A) (a–d) Schematic illustration of design and application of LWIR optical materials. The present work focuses on scheme (a) for creating the IR simulation library starting from 35,238 molecules and scheme (b) for designing LWIR monomers. (B) Illustration of the strategy followed for the computational design protocol of LWIR transparent molecules (wT denotes the LWIR window transmittance value).

Despite the extensive synthetic work in this area, the development of new chalcogenide hybrid polymers with improved IR optical properties remains challenging due to the limited number of organic molecules and materials with high LWIR transmittance.²⁶ We previously reported on the concept of “IR fingerprint engineering” by harnessing the power of DFT calculations to model the fundamental vibrational frequencies and absorptivities of organic and organosulfur model compounds.¹⁶ This led to the development of “NBD2” and poly(sulfur-random-NBD2) which exhibits an attractive suite of thermomechanical and optical properties versus related chalcogenide hybrid polymers, particularly for use in the fabrication of LWIR plastic optic lenses.¹⁶ We recently demonstrated both the fabrication and room temperature LWIR imaging with plastic lenses made

from poly(*S*-*r*-NBD2), which validated the potential of computational chemical methods to accelerate LWIR polymeric materials discovery. Herein, our aim is to develop a protocol capable of simulating IR spectra across a large chemical space; this protocol is exploited for rational design of transparent hydrocarbon molecules with low IR absorbance in the 800–1250 cm^{-1} energy range^{10,27} while satisfying elemental factors for polymerization with sulfur (Figure 1).

We report an automated workflow that uses DFT calculations to create a library (Figure 1A-a) of simulated IR spectra and related LWIR transmittance for 31,570 organic model compounds of varying carbon skeletal size (C_2-C_{10}), along with rapid screening to propose novel candidate molecules (Figure 1A-b). This original high-throughput computational screening approach enables the search and

identification of hydrocarbon molecules exhibiting high transmittance in the LWIR region and is a new tool for IR polymer materials discovery. Those molecules identified with relatively high IR transparencies provide guidelines for the design of new hybrid polymeric materials with enhanced LWIR transparency. A more complete model of the material after polymerization with sulfur would include the effects of sulfur addition to the monomer and intermolecular interactions. However, transparency of the monomer generally decreases when polymerized with sulfur, so monomers with inherently low transparency are unlikely to be appropriate for LWIR optics when polymerized and can be rapidly discarded.¹⁶ From a materials standpoint, the design of organic comonomers is crucial in tailoring the thermomechanical properties and optical transparency of high refractive index polymers from reaction with elemental sulfur (Figure 1A-c). By leveraging these computational methods, materials can be designed and optimized for enhanced optical properties, enabling them to be potentially integrated seamlessly into IR imaging devices (Figure 1A-d).

In this work, we systematically extend previous attempts to understand the complex spectral absorptivity features of molecules in the LWIR region, as well as their derived transparency and compatibility in sulfur polymerization. Previous efforts were limited to the design of NBD2¹⁶ for a copolymerization purpose and the study of IR spectra of a few π -conjugated carbon materials.²⁸ Hence, our approach has both fundamental chemistry and computational appeal and opens new possibilities for accelerated IR imaging materials development.

To build our library, we started with hydrocarbons due to the demonstrated simple spectra in the fingerprint region in the case of organic polymers based on aliphatic structures.^{12,16} Furthermore, this data set offers significant value as simple hydrocarbon-based polymers such as polyethylene (PE) and cyclic olefin polymer (COP) are used for LWIR applications.^{12,16} To this end, we selected a subclass of the generated databases (GDBs)^{29,30} by Reymond and co-workers, referred to as GDB-11. GDB-11 incorporates small organic molecules having up to 11 atoms of carbon, nitrogen, oxygen, or fluorine described via the SMILES³¹ representation, which is a common text encoding used for molecules. All the molecules in the GDB-11 bank follow the rules expressing chemical stability and synthetic feasibility. Our data set includes 27,845 hydrocarbons with ten carbon atoms; 5,714 hydrocarbons with nine carbon atoms; 1,274 hydrocarbons with eight carbon atoms; 290 hydrocarbons with seven carbon atoms; and 115 hydrocarbons with two to six carbon atoms. The selected molecules are charge neutral, closed-shell, and—to provide the possibility to react with sulfur via inverse vulcanization—unsaturated. They include no “heavy” atoms other than carbon. We note that the addition of heteroatoms (N, O, halides, etc.) are less likely to lead to highly IR transparent molecules due to their increased dipole moments. The database includes bicyclic (bridged, fused), tricyclic, or polycyclic structures. The selected 35,238 SMILES are exploited in our computational workflow as explained in the following section.

We carried out density functional theory (DFT) calculations with the B3LYP functional^{32–34} and the 6-31g(d,p) basis set to simulate the IR spectra (both transition energies and absorption intensities) of the molecules.¹⁶ A number of studies have indicated indeed the reliability of calculations at that level

to describe the vibrational properties of organic molecules.^{28,35,36} All DFT calculations were performed with the Gaussian16 package.³⁷ Considering the successfully converged DFT B3LYP calculations and proceeding through the various steps in our workflow, we ended up with the molar absorptivity IR spectra (and LWIR transmittance values) and the corresponding LWIR window transparency (wT) values of 31,570 molecules.

Our procedure is based on the workflow shown in Figure 2 that was automated via python scripts. The steps are as follows:

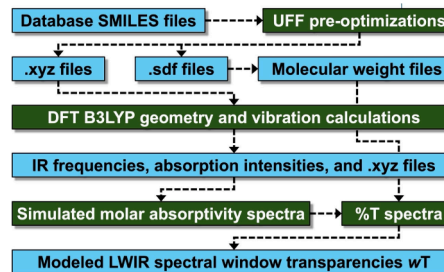


Figure 2. Computational workflow to produce the data set, from molecule enumeration to high-throughput DFT calculations to generate the geometry-optimized molecules, the IR vibrational frequencies and IR intensities, the molar absorptivity and %T transmission spectra, and the corresponding LWIR spectral window transparencies wT .

- (1) The SMILE representations of the molecules are used to generate the corresponding initial preoptimized .xyz geometries using the universal force field (UFF), as implemented in RDKit.³⁸
- (2) The .xyz geometries are used to generate .sdf coordinates using the OpenBabel software³⁹ from which molecular weights are obtained for the determination of the molar concentration in hybrid materials with a 30/70 wt % organic/sulfur composition (see below).
- (3) The UFF preoptimized .xyz geometries are the starting point for the B3LYP/6-31g(d,p) geometry optimizations and vibrational-frequency calculations. In this step, the harmonic vibrational frequencies and absorption intensities of the molecules are determined.
- (4) The resulting full frequency and absorption intensity information is then taken to generate the B3LYP-calculated IR molar absorptivity spectra for each molecule. To broaden the computed stick-like spectra, we use a Lorentzian band shape with a γ (half-width at half-height) value of 5 cm^{-1} , for which the molar absorption coefficient is given as⁴⁰

$$e(\nu) = \frac{1}{1000 \ln(10)\pi} \sum_i \frac{\nu}{\nu_i} \frac{I_i \gamma}{(\nu - \nu_i)^2 + \gamma^2}$$

Here, the i subscript refers to a given normal mode; ν_i (cm^{-1}) and I_i (cm mol^{-1}) are the frequency and the IR intensity of the normal mode, respectively. We store the molar absorbance spectra with 1801 frequency points evenly spaced by 2 cm^{-1} between 400 and $4,000 \text{ cm}^{-1}$. This spacing was found to be sufficient for the numerical determination of the window transparency.

- (5) Given the fact that the hydrocarbon molecules will eventually react with sulfur to form a polymeric thin film

with a high degree of sulfur (which is done to maximize the film index of refraction), we consider a typical composition of the hybrid material to be 30% hydrocarbon and 70% sulfur with a polymer density of 1.7 g/cm³.¹⁶ As in the earlier reports, the material thickness was set to 1 mm.^{12,16} By way of Beer's law, each absorptivity point in the molar absorption spectrum is multiplied by the molar concentration of the organic molecule in the hybrid material and the material thickness to obtain the absorbance spectrum of the material. The absorbance spectrum is then converted to the percent transmission spectrum (%T) where each spectrum point represents the percent transmission at that frequency. The window transparency (*wT*) values reported below correspond to the normalized integrated transmittance in the LWIR window between 800 and 1250 cm⁻¹. In simple terms, *wT* is the average percent transmission across the spectral window.

Our work thus established a protocol, as illustrated in Figures 1B and 2, for screening and identifying the top LWIR transmissive hydrocarbon molecules so as to ascertain structure–property relations for LWIR transparency. We built a library of DFT/B3LYP IR spectra and LWIR spectral window transparencies *wT* for 31,570 hydrocarbon molecules containing from 1 to 10 carbon atoms. The distribution of the computed *wT* values for the whole data set is given in Figure 3a. The corresponding median is 15% with most of the molecules having a *wT* value between 5% and 30%. A low *wT* value naturally points to molecules whose chemical structure/architecture leads to significant vibrational absorptions in the LWIR region. In considering synthetic candidates, a top subclass of molecules exhibiting LWIR *wT* values above 45% was selected to identify the functional groups that are silent in the LWIR spectral window; some representative of these molecules shown in Figure 3b (see also Figure S1 in the Supporting Information) include examples of alkynes, conjugated alkynes, cycloalkenes, propellane moieties, and nonalkynes such as aromatic compounds, cycloolefins, bicyclic compounds, and alicyclic compounds.

As seen from Figure 3b, compound 1, bicyclo[3.3.0]oct-1(5)-ene, has an especially large *wT* value. Since this molecule only incorporates eight carbons, its boiling point (157.4 ± 7.0 °C at 760 mmHg) turns out to be too low to be suitable for inverse vulcanization polymerization, which takes place in the 165–185 °C range.¹⁷ The larger molecules with *wT* values over 50% typically incorporate one or two carbon triple bonds; while alkyne-based cross-linkers such as 1,3-diethynylbenzene (DEB),⁴¹ 1,4-diphenylbutadiyne (DiPhDY),⁴² and diphenylacetylene (DPA)⁴³ have been reported in the literature, the exploitation of triple-bond-containing molecules to produce sulfur/organic hybrid polymers for IR imaging applications has not been studied in detail yet.

It is worth keeping in mind, however, that having relatively high LWIR *wT* values in the selected molecules does not guarantee the retention of reactive groups suitable for polymerization with sulfur. Nonetheless, we can still gain insight into potential candidates for LWIR applications by imposing some semiempirical structural constraints on molecules from the full DFT library. In particular, we can generate *focused libraries* that utilize and compare specifically chosen molecular architectures and then evaluate similar molecules versus their respective LWIR *wT*.

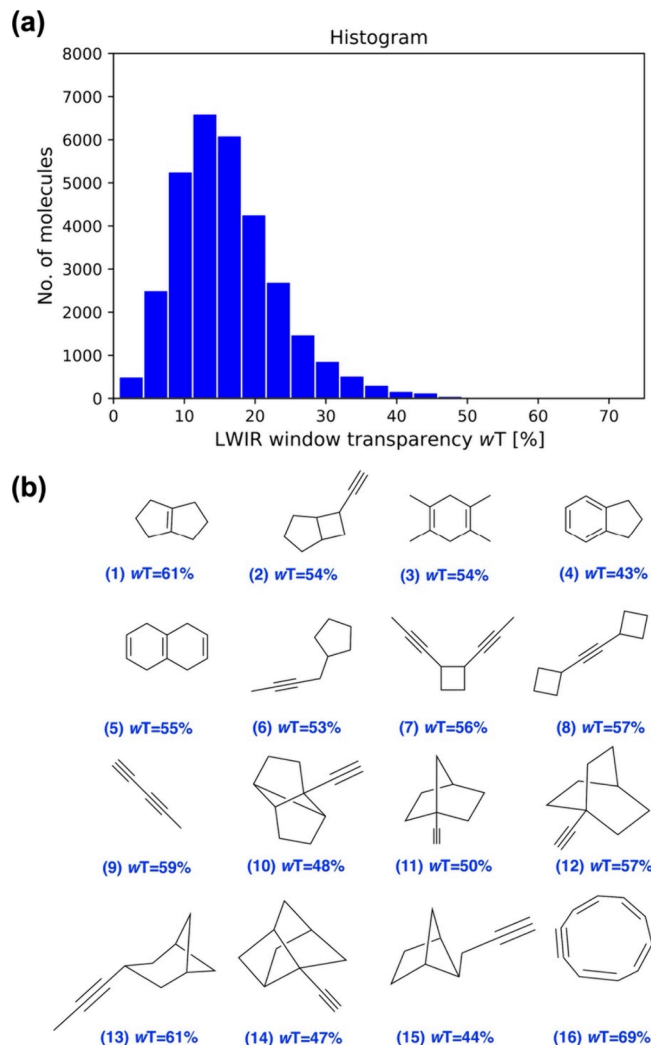


Figure 3. (a) Distribution of the LWIR window transparency (*wT*) values for the whole data set, based on the B3LYP DFT spectra for 1 mm thick organic/sulfur hybrid materials with 30/70 wt % composition. (b) Representative structures with calculated window transparency (*wT*) values above 45% in the LWIR 800–1250 cm⁻¹ energy window for 1 mm thick organic/sulfur hybrid materials with 30/70 wt % composition.

To date, the organic comonomers that have been studied for the inverse vulcanization process contain C=C groups.^{11,44–46} For the focused library shown in Figure 4a, we started with an actual known cyclic olefin of relevance to inverse vulcanization, norbornadiene (compound 17 in Figure 4a, NBD) and extracted 14 similar compounds retaining similar molecular formula and cyclopropellane architecture. The DFT IR simulation of NBD gives a high *wT* of 39%, which examination of these related 14 molecules confirm promising LWIR *wT* values between 28% and 45% with the presence of at least one vinylene functionality. As illustrated in Figure 4b, these molecules show indeed only very weak absorptions in the 800–1250 cm⁻¹ energy range. Several of these molecules (17, 23, 25, and 27) contain two C=C groups while molecules 22 and 26 possess three C=C groups. Such structures thus provide for more linkage points with sulfur chains in the course of inverse vulcanization, since the polymerization process leads to breakage of the C=C double bonds and formation of C–S bonds;^{16,17} given that both C=C and C–S bonds have

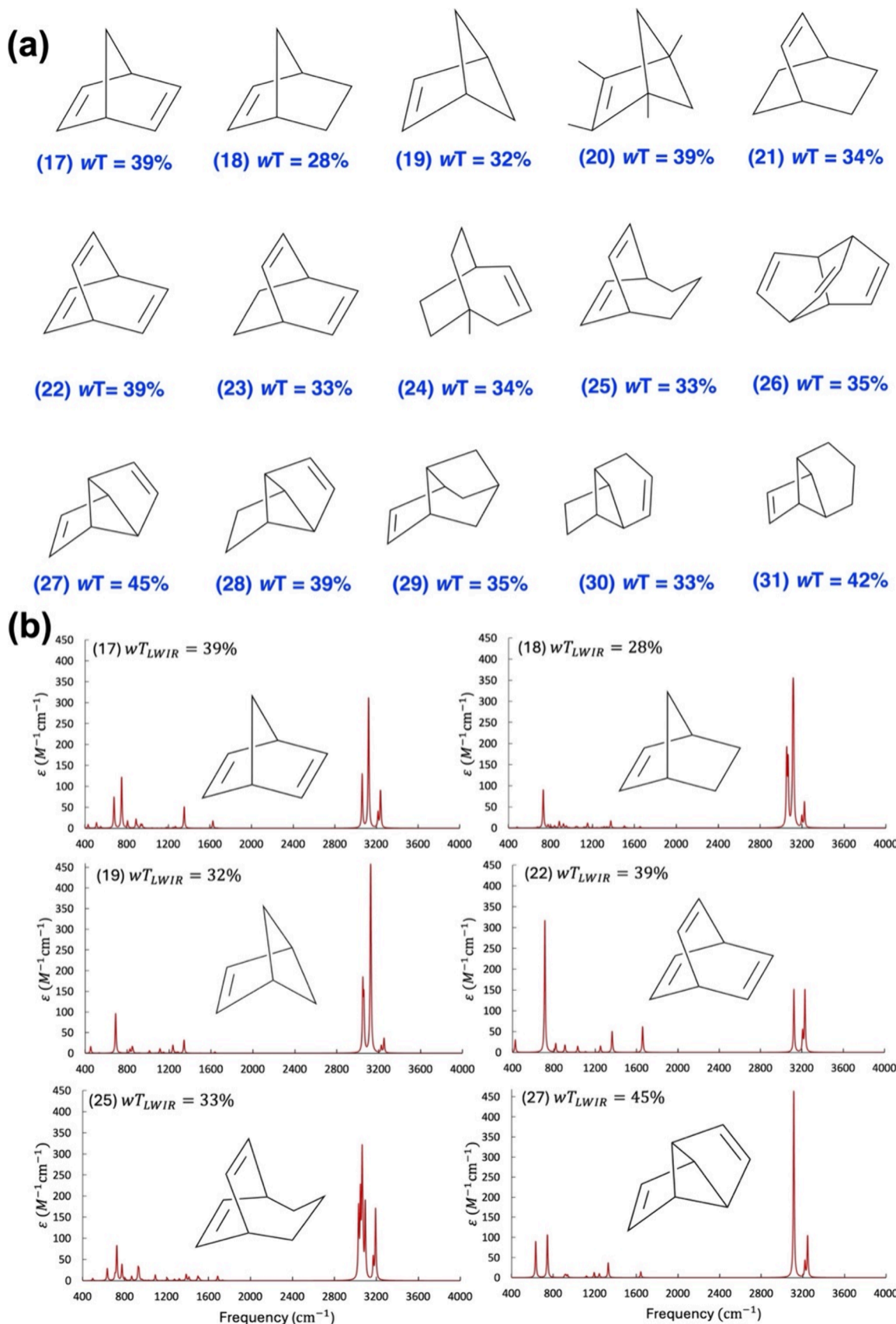


Figure 4. (a) Illustration of building-block candidates with a large LWIR window of transmittance ($800\text{--}1250\text{ cm}^{-1}$, 1 mm thick organic/sulfur hybrid materials with 30/70 wt % composition) suitable for inverse vulcanization with elemental sulfur. (b) Calculated IR spectra of selected comonomers extracted from (a). A Lorentzian band shape with a γ (half-width at half-height) value of 5 cm^{-1} is used to broaden the computed transitions. Absorptivities in the LWIR region for those molecules are determined to be indeed very low.

negligible activity in the LWIR region, we do not expect any significant changes to the wT values reported here upon copolymerization with elemental sulfur.

As mentioned above, the temperatures commonly used for inverse vulcanization range from 165 to 185 °C. Therefore, a suitable boiling point is also an important condition in the selection of organic comonomers. For instance, while NBD has been of initial interest in the design of LWIR materials,¹⁶ its volatility (boiling point of ~89 °C) prevented its effective use in inverse vulcanization. To solve this problem, a dimer of NBD containing 14 carbon atoms (compound 44, NBD2, see Figure 5) was considered instead (we note that a compromise

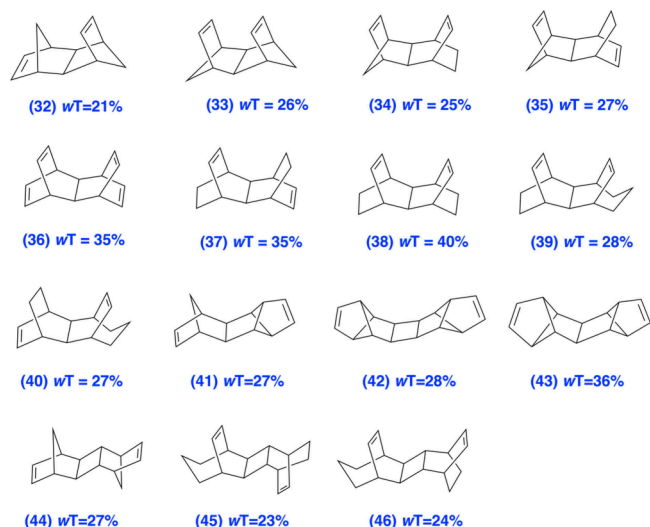


Figure 5. Illustration of comonomers designed on the basis of the building blocks of Figure 4a, as potential candidates for inverse vulcanization with elemental sulfur. The wT values indicate the window transparency in the LWIR frequency window for 1 mm thick organic/sulfur hybrid materials with 30/70 wt % composition.

has to be reached between decreasing the volatility and increasing the molecular size of the organic comonomer since the sulfur fraction of the eventual sulfur-hydrocarbon polymer should be maximized).¹⁶ While we have investigated molecules with only up to ten carbon atoms, meaning that it remains unclear how many of the best-performing molecules discussed above actually satisfy the volatility condition, the issue can be overcome by building up strategically somewhat larger molecules as was considered in the case of NBD2. A simple way to do so is to generate new molecules by fusing some of the building blocks shown in Figure 4a. A set of molecules obtained in this way is shown in Figure 5.

As seen from Figure 5, by fusing two NBD units, we obtain the two stillene structures 32 and 33, which incorporate 12 carbons (it is interesting to mention that the radical-cations of 32 and 33 and their derivatives have been intensively investigated in the 1980s and 1990s in the context of intramolecular electron transfer⁴⁷). While the wT values of these stillenes are reduced in comparison to that of NBD, they are comparable to that of NBD2. In fact, more promising results are obtained if, instead of NBD units, [2.2.2]propellane structural motifs (21-23) are used as building blocks. Indeed, compound 38 obtained in this way exhibits a wT value of 40% that is nearly twice as large as those of the NBD-based compounds. Also, molecule 36, while having a slightly smaller

wT value of 35%, affords four C=C bonds that can be exploited in the polymerization with elemental sulfur. The comparison of the IR absorption spectra of the fused [2.2.2]propellane systems with those of the parent fragments (see Figure S2) indicates that they are nearly identical. Thus, compounds 36 and 38 appear to be great candidates to develop hybrid sulfur/organic polymers with large sulfur-to-carbon ratios.

While very promising, these results call for a more systematic study of other unsaturated hydrocarbons containing 11 to 14 carbon atoms, using either the high-throughput screening approach developed here or a machine learning methodology. Work along those lines is now in progress in our laboratories.

In search of new hydrocarbon molecules appropriate for the development of hybrid sulfur-organic polymeric materials relevant to long-wavelength IR (LWIR) imaging, we developed a high-throughput computational screening approach based on DFT/B3LYP calculations of the molar absorptivities in the LWIR region of the corresponding LWIR spectral window transparencies, wT . We applied our high-throughput protocol to a relatively large chemical space of hydrocarbons consisting of 31,570 molecules, which enabled us to create a library including a series of organic molecules exhibiting high transmittance in the LWIR energy region.

We identified building blocks with very low vibrational absorptions in the LWIR domain and containing at least one C=C group, from which we were able to design a set of compounds illustrated in Figure 5 with high LWIR transmittance values and expected low volatility. These compounds are promising candidates as hydrocarbon component of sulfur/organic plastics for optical applications.

■ ASSOCIATED CONTENT

Data Availability Statement

All data needed to evaluate the conclusions in the paper are presented within the paper and/or the Supporting Information. Additional data, including the list of SMILES strings, optimized XYZ coordinates used to simulate the DFT molar absorptivity IR spectra, and the related spectra underlying this study, are available at Zenodo⁴⁸ [10.5281/zenodo.13163525]

■ Supporting Information

The Supporting Information is available free of charge at <https://pubs.acs.org/doi/10.1021/acsmaterialslett.4c01037>.

(Chemical structures of hydrocarbons with window transparency (wT) values above 45% in the LWIR 800–1250 cm^{-1} energy window; calculated IR spectra of the designed comonomers given in Figure 5 (PDF)

■ AUTHOR INFORMATION

Corresponding Authors

Veaceslav Coropceanu – Department of Chemistry and Biochemistry, The University of Arizona, Tucson, Arizona 85721, United States; Email: coropceanu@arizona.edu

Jeffrey Pyun – Department of Chemistry and Biochemistry and James Wyant College of Optical Sciences, The University of Arizona, Tucson, Arizona 85721, United States; Email: jpyun@arizona.edu

Dennis L. Lichtenberger – Department of Chemistry and Biochemistry, The University of Arizona, Tucson, Arizona 85721, United States; Email: dlichten@arizona.edu

Jean-Luc Brédas – Department of Chemistry and Biochemistry, The University of Arizona, Tucson, Arizona

85721, United States;  orcid.org/0000-0001-7278-4471;
Email: jlbredas@arizona.edu

Authors

Maliheh Shaban Tameh – Department of Chemistry and Biochemistry, The University of Arizona, Tucson, Arizona 85721, United States;  orcid.org/0000-0002-8259-8637

Addison G. Coen – Department of Chemistry and Biochemistry, The University of Arizona, Tucson, Arizona 85721, United States;  orcid.org/0000-0001-8728-7654

Complete contact information is available at:
<https://pubs.acs.org/10.1021/acsmaterialslett.4c01037>

Author Contributions

CRediT: **Maliheh Shaban Tameh** conceptualization, data curation, formal analysis, investigation, methodology, validation, visualization, writing-original draft, writing-review & editing; **Veaceslav Coropceanu** conceptualization, formal analysis, investigation, methodology, project administration, supervision, validation, visualization, writing-review & editing; **Addison Gray Coen** formal analysis, methodology; **Jeffrey Pyun** conceptualization, validation, visualization, writing-review & editing; **Dennis L. Lichtenberger** conceptualization, data curation, formal analysis, funding acquisition, methodology, resources, validation, visualization, writing-review & editing; **Jean-Luc Bredas** conceptualization, funding acquisition, methodology, project administration, resources, supervision, validation, writing-review & editing.

Notes

The authors declare no competing financial interest.

ACKNOWLEDGMENTS

This work was funded by the National Science Foundation and the Air Force Research Laboratory through DMREF-2118578. The authors are thankful for the use of the High Performance Computing (HPC) resources supported by the University of Arizona TRIF, UITS, and Research, Innovation, and Impact (RII) Offices and maintained by the Research Technologies Department.

REFERENCES

- (1) Akula, A.; Ghosh, R.; Sardana, H. Thermal imaging and its application in defence systems. In *AIP conference proceedings*; American Institute of Physics, 2011; Vol. 1391, pp 333–335.
- (2) Razeghi, M.; Nguyen, B.-M. Advances in mid-infrared detection and imaging: a key issues review. *Rep. Prog. Phys.* **2014**, *77* (8), No. 082401.
- (3) Ioannou, S.; Gallese, V.; Merla, A. Thermal infrared imaging in psychophysiology: potentialities and limits. *Psychophysiology* **2014**, *51* (10), 951–963.
- (4) Nguyen, T. X. B.; Rosser, K.; Chahl, J. A review of modern thermal imaging sensor technology and applications for autonomous aerial navigation. *J. Imaging* **2021**, *7* (10), 217.
- (5) Farooq, M. A.; Shariff, W.; O'callaghan, D.; Merla, A.; Corcoran, P. On the role of thermal imaging in automotive applications: A critical review. *IEEE Access* **2023**, *11*, 25152–25173.
- (6) Nishant, A.; Kim, K. J.; Showghi, S. A.; Himmelhuber, R.; Kleine, T. S.; Lee, T.; Pyun, J.; Norwood, R. A. High refractive index chalcogenide hybrid inorganic/organic polymers for integrated photonics. *Adv. Opt. Mater.* **2022**, *10* (16), 2200176.
- (7) Liu, J.-g.; Ueda, M. High refractive index polymers: fundamental research and practical applications. *J. Mater. Chem.* **2009**, *19* (47), 8907–8919.
- (8) Higashihara, T.; Ueda, M. Recent progress in high refractive index polymers. *Macromolecules* **2015**, *48* (7), 1915–1929.
- (9) Kang, K.-S.; Olikagu, C.; Lee, T.; Bao, J.; Molineux, J.; Holmen, L. N.; Martin, K. P.; Kim, K.-J.; Kim, K. H.; Bang, J.; et al. Sulfenyl chlorides: An alternative monomer feedstock from elemental sulfur for polymer synthesis. *J. Am. Chem. Soc.* **2022**, *144* (50), 23044–23052.
- (10) Lee, T.; Dirlam, P. T.; Njardarson, J. T.; Glass, R. S.; Pyun, J. Polymerizations with elemental sulfur: from petroleum refining to polymeric materials. *J. Am. Chem. Soc.* **2022**, *144* (1), 5–22.
- (11) Zhang, Y.; Glass, R. S.; Char, K.; Pyun, J. Recent advances in the polymerization of elemental sulphur, inverse vulcanization and methods to obtain functional Chalcogenide Hybrid Inorganic/Organic Polymers (CHIPS). *Polym. Chem.* **2019**, *10* (30), 4078–4105.
- (12) Kleine, T. S.; Glass, R. S.; Lichtenberger, D. L.; Mackay, M. E.; Char, K.; Norwood, R. A.; Pyun, J. 100th Anniversary of Macromolecular Science Viewpoint: High Refractive Index Polymers from Elemental Sulfur for Infrared Thermal Imaging and Optics. *ACS Macro Lett.* **2020**, *9* (2), 245–259.
- (13) Boyd, D.; Baker, C.; Myers, J.; Nguyen, V.; Drake, G.; McClain, C.; Kung, F.; Bowman, S.; Kim, W.; Sanghera, J. ORMOCHALCs: organically modified chalcogenide polymers for infrared optics. *Chem. Commun.* **2017**, *53* (1), 259–262.
- (14) Boyd, D. A.; Nguyen, V. Q.; McClain, C. C.; Kung, F. H.; Baker, C. C.; Myers, J. D.; Hunt, M. P.; Kim, W.; Sanghera, J. S. Optical properties of a sulfur-rich organically modified chalcogenide polymer synthesized via inverse vulcanization and containing an organometallic comonomer. *ACS Macro Lett.* **2019**, *8* (2), 113–116.
- (15) Crockett, M. P.; Evans, A. M.; Worthington, M. J.; Albuquerque, I. S.; Slattery, A. D.; Gibson, C. T.; Campbell, J. A.; Lewis, D. A.; Bernardes, G. J.; Chalker, J. M. Sulfur-Limonene Polysulfide: A Material Synthesized Entirely from Industrial By-Products and Its Use in Removing Toxic Metals from Water and Soil. *Angew. Chem., Int. Ed.* **2016**, *55* (5), 1714–1718.
- (16) Kleine, T. S.; Lee, T.; Carothers, K. J.; Hamilton, M. O.; Anderson, L. E.; Ruiz Diaz, L.; Lyons, N. P.; Coasey, K. R.; Parker, W. O., Jr.; Borghi, L.; et al. Infrared Fingerprint Engineering: A Molecular-Design Approach to Long-Wave Infrared Transparency with Polymeric Materials. *Angew. Chem., Int. Ed.* **2019**, *58* (49), 17656–17660.
- (17) Chung, W. J.; Griebel, J. J.; Kim, E. T.; Yoon, H.; Simmonds, A. G.; Ji, H. J.; Dirlam, P. T.; Glass, R. S.; Wie, J. J.; Nguyen, N. A.; et al. The use of elemental sulfur as an alternative feedstock for polymeric materials. *Nat. Chem.* **2013**, *5* (6), 518–524.
- (18) Kleine, T. S.; Nguyen, N. A.; Anderson, L. E.; Namnabat, S.; LaVilla, E. A.; Showghi, S. A.; Dirlam, P. T.; Arrington, C. B.; Manchester, M. S.; Schwiegerling, J.; et al. High refractive index copolymers with improved thermomechanical properties via the inverse vulcanization of sulfur and 1, 3, 5-triisopropenylbenzene. *ACS Macro Lett.* **2016**, *5* (10), 1152–1156.
- (19) Griebel, J. J.; Nguyen, N. A.; Namnabat, S.; Anderson, L. E.; Glass, R. S.; Norwood, R. A.; Mackay, M. E.; Char, K.; Pyun, J. Dynamic covalent polymers via inverse vulcanization of elemental sulfur for healable infrared optical materials. *ACS Macro Lett.* **2015**, *4* (9), 862–866.
- (20) Wu, X.; Smith, J. A.; Petcher, S.; Zhang, B.; Parker, D. J.; Griffin, J. M.; Hasell, T. Catalytic inverse vulcanization. *Nat. Commun.* **2019**, *10* (1), 647.
- (21) Smith, J. A.; Wu, X.; Berry, N. G.; Hasell, T. High sulfur content polymers: the effect of crosslinker structure on inverse vulcanization. *J. Polym. Sci., Part A: Polym. Chem.* **2018**, *56* (16), 1777–1781.
- (22) Kang, K. S.; Iyer, K. A.; Pyun, J. On the fundamental polymer chemistry of inverse vulcanization for statistical and segmented copolymers from elemental sulfur. *Chem. - Eur. J.* **2022**, *28* (35), No. e202200115.
- (23) Smith, J. A.; Green, S. J.; Petcher, S.; Parker, D. J.; Zhang, B.; Worthington, M. J.; Wu, X.; Kelly, C. A.; Baker, T.; Gibson, C. T.; et al. Crosslinker copolymerization for property control in inverse vulcanization. *Chem. - Eur. J.* **2019**, *25* (44), 10433–10440.

(24) Arslan, M.; Kiskan, B.; Cengiz, E. C.; Demir-Cakan, R.; Yagci, Y. Inverse vulcanization of bismaleimide and divinylbenzene by elemental sulfur for lithium sulfur batteries. *Eur. Polym. J.* **2016**, *80*, 70–77.

(25) Hwang, J. H.; Kim, S. H.; Cho, W.; Lee, W.; Park, S.; Kim, Y. S.; Lee, J. C.; Lee, K. J.; Wie, J. J.; Kim, D. G. A Microphase Separation Strategy for the Infrared Transparency-Thermomechanical Property Conundrum in Sulfur-Rich Copolymers. *Adv. Opt. Mater.* **2023**, *11* (5), 2202432.

(26) Anderson, L. E.; Kleine, T. S.; Zhang, Y.; Phan, D. D.; Namnabat, S.; LaVilla, E. A.; Konopka, K. M.; Ruiz Diaz, L.; Manchester, M. S.; Schwiegerling, J.; et al. Chalcogenide hybrid inorganic/organic polymers: Ultrahigh refractive index polymers for infrared imaging. *ACS Macro Lett.* **2017**, *6* (5), 500–504.

(27) Arouh, S.; Nishant, A.; Pyun, J.; Norwood, R. A. Characterization of the optical and electronic properties of chalcogenide hybrid inorganic/organic polymer thin films. *Opt. Mater. Express* **2023**, *13* (10), 2737–2745.

(28) Cho, E.; Pratik, S. M.; Pyun, J.; Coropceanu, V.; Brédas, J. L. π -Conjugated Carbon-Based Materials for Infrared Thermal Imaging. *Adv. Opt. Mater.* **2023**, *11* (12), 2300029.

(29) Blum, L. C.; Reymond, J.-L. 970 million druglike small molecules for virtual screening in the chemical universe database GDB-13. *J. Am. Chem. Soc.* **2009**, *131* (25), 8732–8733.

(30) Ruddigkeit, L.; Van Deursen, R.; Blum, L. C.; Reymond, J.-L. Enumeration of 166 billion organic small molecules in the chemical universe database GDB-17. *J. Chem. Inf. Model.* **2012**, *52* (11), 2864–2875.

(31) Weininger, D. SMILES, a chemical language and information system. 1. Introduction to methodology and encoding rules. *J. Chem. Inf. Comput. Sci.* **1988**, *28* (1), 31–36.

(32) Becke, A. D. Density-functional thermochemistry. I. The effect of the exchange-only gradient correction. *J. Chem. Phys.* **1992**, *96* (3), 2155–2160.

(33) Lee, C.; Yang, W.; Parr, R. G. Development of the Colle-Salvetti correlation-energy formula into a functional of the electron density. *Phys. Rev. B* **1988**, *37* (2), 785.

(34) Tirado-Rives, J.; Jorgensen, W. L. Performance of B3LYP density functional methods for a large set of organic molecules. *J. Chem. Theory Comput.* **2008**, *4* (2), 297–306.

(35) Bauschlicher, C. W., Jr; Hudgins, D. M.; Allamandola, L. J. The infrared spectra of polycyclic aromatic hydrocarbons containing a five-membered ring: symmetry breaking and the B3LYP functional. *Theor. Chem. Acc.* **1999**, *103*, 154–162.

(36) Fuente, E.; Menéndez, J.; Díez, M.; Suárez, D.; Montes-Morán, M. Infrared spectroscopy of carbon materials: a quantum chemical study of model compounds. *J. Phys. Chem. B* **2003**, *107* (26), 6350–6359.

(37) Frisch, M. J.; Trucks, G. W.; Schlegel, H. B.; Scuseria, G. E.; Robb, M. A.; Cheeseman, J. R.; Scalmani, G.; Barone, V.; Petersson, G. A.; Nakatsuji, H.; Li, X.; Caricato, M.; Marenich, A. V.; Bloino, J.; Janesko, B. G.; Gomperts, R.; Mennucci, B.; Hratchian, H. P.; Ortiz, J. V.; Izmaylov, A. F.; Sonnenberg, J. L.; Williams, D.; Ding, F.; Lipparini, F.; Egidi, F.; Goings, J.; Peng, B.; Petrone, A.; Henderson, T.; Ranasinghe, D.; Zakrzewski, V. G.; Gao, J.; Rega, N.; Zheng, G.; Liang, W.; Hada, M.; Ehara, M.; Toyota, K.; Fukuda, R.; Hasegawa, J.; Ishida, M.; Nakajima, T.; Honda, Y.; Kitao, O.; Nakai, H.; Vreven, T.; Throssell, K.; Montgomery, Jr., J. A.; Peralta, J. E.; Ogliaro, F.; Bearpark, M. J.; Heyd, J. J.; Brothers, E. N.; Kudin, K. N.; Staroverov, V. N.; Keith, T. A.; Kobayashi, R.; Normand, J.; Raghavachari, K.; Rendell, A. P.; Burant, J. C.; Iyengar, S. S.; Tomasi, J.; Cossi, M.; Millam, J. M.; Klene, M.; Adamo, C.; Cammi, R.; Ochterski, J. W.; Martin, R. L.; Morokuma, K.; Farkas, O.; Foresman, J. B.; Fox, D. J. *Gaussian 16 Rev. C.01*; Gaussian Inc.: Wallingford, CT, 2016.

(38) Landrum, G. RDKit: open-source cheminformatics. <https://www.rdkit.org/>.

(39) O'Boyle, N. M.; Banck, M.; James, C. A.; Morley, C.; Vandermeersch, T.; Hutchison, G. R. Open Babel: An open chemical toolbox. *J. Cheminf.* **2011**, *3*, 1–14.

(40) Kawiecki, R. W.; Devlin, F.; Stephens, P.; Amos, R.; Handy, N. Vibrational circular dichroism of propylene oxide. *Chem. Phys. Lett.* **1988**, *145* (5), 411–417.

(41) Sun, Z.; Xiao, M.; Wang, S.; Han, D.; Song, S.; Chen, G.; Meng, Y. Sulfur-rich polymeric materials with semi-interpenetrating network structure as a novel lithium–sulfur cathode. *J. Mater. Chem. A* **2014**, *2* (24), 9280–9286.

(42) Dirlam, P. T.; Simmonds, A. G.; Kleine, T. S.; Nguyen, N. A.; Anderson, L. E.; Klever, A. O.; Florian, A.; Costanzo, P. J.; Theato, P.; Mackay, M. E.; et al. Inverse vulcanization of elemental sulfur with 1, 4-diphenylbutadiyne for cathode materials in Li–S batteries. *RSC Adv.* **2015**, *5* (31), 24718–24722.

(43) Park, K. W. *The inverse vulcanisation of siloxane and alkyne cross-linkers with sulfur*. Ph.D. Thesis, The University of Auckland, New Zealand, 2023. (Available to download from <https://researchspace.auckland.ac.nz/bitstream/handle/2292/66024/Park-2023-thesis.pdf?sequence=4>).

(44) Griebel, J. J.; Glass, R. S.; Char, K.; Pyun, J. Polymerizations with elemental sulfur: A novel route to high sulfur content polymers for sustainability, energy and defense. *Prog. Polym. Sci.* **2016**, *58*, 90–125.

(45) Worthington, M. J.; Kucera, R. L.; Chalker, J. M. Green chemistry and polymers made from sulfur. *Green Chem.* **2017**, *19* (12), 2748–2761.

(46) Chalker, J. M.; Worthington, M. J.; Lundquist, N. A.; Eadsdale, L. J. Synthesis and applications of polymers made by inverse vulcanization. *Sulfur Chemistry* **2019**, 125–151.

(47) Jordan, K. D.; Paddon-Row, M. N. Analysis of the interactions responsible for long-range through-bond-mediated electronic coupling between remote chromophores attached to rigid polynorbornyl bridges. *Chem. Rev.* **1992**, *92* (3), 395–410.

(48) Tameh, M. S.; Coropceanu, V.; Coen, A. G.; Pyun, J.; Lichtenberger, D. L.; Brédas, J.-L. High-throughput Computational Screening of Hydrocarbon Molecules for Long-wavelength Infrared Imaging. *Data set*. Zenodo **2024**. DOI: [10.5281/zenodo.13163525](https://doi.org/10.5281/zenodo.13163525).